Published in : NeuroImage (2011), vol. 57, pp. 198-205.
Status : Postprint (Author's version)

Brain functional integration decreases during propofol-induced loss of consciousness

Jessica Schrouff[a], Vincent Perlbarg[b], Melanie Boly[a], Guillaume Marrelec[b], Pierre Boveroux[a], Audrey Vanhaudenhuyse[a], Marie-Aurelie Bruno[a], Steven Laureys[a], Christophe Phillips[a], Melanie Pélégrini-Issac[b], Pierre Maquet[a], Habib Benali[b]

[a] *Cyclotron Research Centre, University of Liège, Liège, Belgium*

[b] *Inserm and UPMC Univ Paris 06, UMR-S 678, Laboratoire d'Imagerie Fonctionnelle, Paris, France*

ABSTRACT

Consciousness has been related to the amount of integrated information that the brain is able to generate. In this paper, we tested the hypothesis that the loss of consciousness caused by propofol anesthesia is associated with a significant reduction in the capacity of the brain to integrate information. To assess the functional structure of the whole brain, functional integration and partial correlations were computed from fMRI data acquired from 18 healthy volunteers during resting wakefulness and propofol-induced deep sedation. Total integration was significantly reduced from wakefulness to deep sedation in the whole brain as well as within and between its constituent networks (or systems). Integration was systematically reduced within each system (i.e., brain or networks), as well as between networks. However, the ventral attentional network maintained interactions with most other networks during deep sedation. Partial correlations further suggested that functional connectivity was particularly affected between parietal areas and frontal or temporal regions during deep sedation. Our findings suggest that the breakdown in brain integration is the neural correlate of the loss of consciousness induced by propofol. They stress the important role played by parietal and frontal areas in the generation of consciousness.

Keywords : Anesthesia ; Propofol ; Networks ; Connectivity ; Quantification ; Integration

Introduction

Why do we lose consciousness under general anesthesia? Oddly enough, this question has received little attention so far. Positron emission tomography studies reported a drop in global brain metabolism to about half of normal values during unconsciousness induced by halothane (Alkire et al., 1999) and propofol (Alkire et al., 1995). Although these results certainly illustrate the profound influence these drugs have on brain function, they do not inform us about the mechanisms underlying the loss of consciousness. Indeed, global brain activity is not necessarily a reliable predictor of individual consciousness. For instance, patients can emerge from a vegetative state and recover consciousness while their global brain metabolism is still dramatically reduced (Laureys et al., 1999). Another hypothesis assumes that general anesthesia hinders the emergence of consciousness because it perturbs the functional interactions between brain areas. This hypothesis has received some experimental support: thalamo-cortical and cortico-cortical connectivity was shown to be variously impaired during isoflurane, halothane (White and Alkire, 2003), propofol (Boveroux et al., 2010; Mhuircheartaigh et al., 2010) and sevoflurane anesthesia (Martuzzi et al., 2010). However, brain connectivity can be disrupted without consciousness being drastically modified (e.g., in early stage of Alzheimer's disease, Greicius et al., 2004; Zhang et al., 2009). This piece of evidence indicates that modifications in brain connectivity are necessary but not always sufficient to account for the loss of consciousness. Still another hypothesis associates consciousness with the capacity of the brain to efficiently integrate information across different specialized subsystems (Tononi, 2005). According to this theory, loss of consciousness during anesthesia could be associated with a loss of brain integration [brain would tend to be organized in distributed independent modules (Alkire et al., 2008)] or to a less likely dissolution of brain specialization (i.e., all brain areas would tend to be homogeneously connected to the rest of the brain). The quantitative assessment of functional brain integration during general anesthesia has never been conducted. The primary aim of the present paper was precisely to quantify the brain functional integration and its main constituent networks during resting wakefulness and general anesthesia induced by propofol. The reason why propofol was chosen for this study is that this particular anesthetic has been shown not

to interfere with regional cerebral blood flow response at sedative concentrations (Veselis et al., 2005), and does not modify flow-metabolism coupling in humans (Johnston et al., 2003). Furthermore, once a target effect-site concentration is reached, propofol allows maintaining a stable unconscious state for several minutes, with only minimal subject movements and without requiring the volunteers' intubation. This renders propofol ideally suited for experiments using resting state fMRI acquisitions.

In addition, some brain areas seem more regularly involved than others in conscious processes. In particular, the recruitment of frontal and parietal associative cortices has repeatedly been associated with conscious representations (Dehaene et al., 2006; Laureys et al., 1999; Rees et al., 2002). These areas are thought to materialize a global workspace in which unified and integrated mental representations reach consciousness (Baars, 2005). The second aim of the present paper was to assess quantitatively the functional integration between frontal and parietal areas during resting wakefulness and general anesthesia.

In this study, fMRI time series acquired during resting wakefulness and deep sedation were analyzed with novel validated methods based on information theory, which allow to compute the hierarchical organization of brain integration (i.e., at the level of the whole brain and its constituent networks). The results indicate a breakdown of functional integration within all brain networks, between most of them and especially between frontal and parietal cortices.

Materials and methods

Population

The data set considered in the present work has already been published in Boveroux et al. (2010). Eighteen healthy volunteers (14 females, mean age: 22.8 years, range: 19-31) participated in the study, which was approved by the Ethics Committee of the Faculty of Medicine of the University of Liege. They were fully informed and gave their written consent. They had no history of medical, neurological or psychiatric disease. None of them was under medication.

Sedation protocol

Anesthesia was achieved with a computer-controlled intravenous infusion of propofol (using a target controlled infusion device, Diprifusor©-algorithm, Pharmacokinetics and Pharmacodynamics Software Server, Department of Anesthesia, Stanford University, USA) to obtain constant effect-site concentrations. Physiological parameters such as blood pressure, cardiac rhythm or pulse oxymetry were monitored.

During functional magnetic resonance imaging (fMRI), the participants' level of consciousness was estimated using the Ramsay scale: the subject was asked a simple task ('squeeze strongly my hand') and his/her level of consciousness was clinically evaluated from the strength and rapidity of his/her response. The volunteer was considered fully awake (stage wakefulness, Ramsay 2) when the response was clear and quick, in mild sedation (stage mild sedation, Ramsay 3) if the response was clear but slow, in deep sedation if there was no response (stage deep sedation, Ramsay 5-6) and in recovery of consciousness (stage recovery, Ramsay 2) when he/she awoke from deep sedation.

fMRI data acquisition

Functional MRI data were acquired on a 3 T Siemens Allegra scanner with a gradient-echo echo-planar imaging sequence using axial slice orientation and covering the whole brain (32 interleaved slices, TR = 2460 ms, TE = 40 ms, FOV = 220 mm, FA = 90°, voxel size = 3.45 × 3.45 × 3 mm, matrix size = 64 × 64 × 32). All subjects had four sessions (one for each level of anesthesia: wakefulness, mild sedation, deep sedation and recovery) of 200 (for 12 volunteers) or 350 (for 6 volunteers) scans each. Only data in full wakefulness and deep sedation were analyzed and are reported here.

Fig. 1. *Three-step procedure used to compute integration and partial correlations at the group level. (1) spatial ICA was applied on each subject, leading to 40 IC (default value). These n*40 IC were then hierarchically clustered and IC corresponding to cardiorespiratory artefacts were discarded. Group t-maps were then computed revealing functional networks at the group level. (2) From these maps, ROIs were automatically selected and used for the computation (3) of integration and partial correlations via a 1000 samples Bayesian numerical sampling scheme of the posterior distribution.*

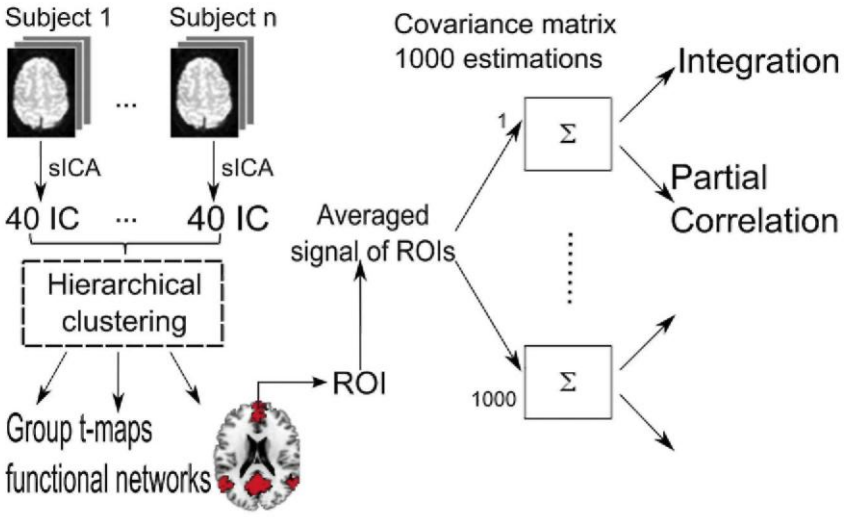

fMRI data connectivity analyses

Functional images were corrected for slice timing and realigned to compensate for within-session rigid movements using the SPM5 software (statistical parametric mapping, www.fil.ion.ucl.ac.uk), independently for each condition.

Functional connectivity between regions of interest was computed following a three-step procedure (Fig. 1) as implemented in the NetBrainWork toolbox (http://sites.google.com/site/netbrainwork). First, the detection of functional networks at the group level was achieved using NEDICA (NEtwork Detection using ICA, Perlbarg et al., 2008), which detected networks at the individual level using spatial independent component analysis (sICA). After registration into the MNI standardized space (using the SPM2 software), a hierarchical clustering was performed on the independent components (IC) from all subjects, yielding a similarity tree. The partitioning of the similarity tree into classes relied on the idea that each class should ideally be composed of one and only one IC from each subject. Two parameters were computed to quantify this idea, which allowed selecting the consistent classes across subjects. A group *t*-map was associated with each selected class (Perlbarg et al., 2008). The group representative classes, the spatial structure of which was characteristic of known functional networks according to the literature, were used for subsequent analysis as the main systems of interest (SOIs). Maps corresponding to noise processes or not characteristic of any previously identified functional network were discarded. Second, 20-voxel regions of interest (ROIs) were selected around the peaks of each group t-map and corresponded to the main nodes of functional networks. Third, we quantified the functional interactions within and between the SOIs using two types of measures, hierarchical integration and partial correlation. As a preprocessing step before the computation of functional interactions, the CORSICA method (CORrection of Structured noise using Spatial Independent Component Analysis, Perlbarg et al., 2007) was used to take physiological noise into account. This technique takes advantage of the fact that the spatial distribution of physiological noise or head motion signals is independent of the TR of the acquisitions. In particular, CSF pools such as the ventricles appear to act as detectors of head motion and physiology-related movements, and the major blood vessels as detectors of cardiac activity. CORSICA includes three successive steps: sICA decomposition, selection of noise-related components using specific masks of interest comprising the ventricles, the brainstem and the basilar arteries, and removal of those components.

Hierarchical integration corresponds to the mutual information between time courses of BOLD signal recorded in the various ROIs (Marrelec et al., 2005, 2009). It provides a global measure of functional information exchanges within and/or between brain systems. Furthermore, if a system is divided into subsystems, the total

integration of this system can be decomposed into within-subsystem and between-subsystem integration (Marrelec et al., 2008). In particular, the total integration of the brain is equal to the sum of within-SOIs integration and between-SOIs integration. To infer the integration measures, a Bayesian numerical sampling scheme approximating the posterior distribution of the parameters of interest in a group analysis is necessary (Marrelec et al., 2006). In the present work, we used 1000 samples to perform this approximation, therefore leading to a thousand estimations of integration measures. The results are presented in terms of the mean and standard deviation of the 1000 estimates. The interested reader can find further information about the concept and the computation of hierarchical integration in Appendices A and B and in Marrelec et al., 2008. Technical details about the computation of statistics on the integration measures can be found in Appendix C.

Since hierarchical integration provides a global measure of interaction, it is unable to quantify pairwise functional connectivity. To do so in a given system, we resorted to partial correlation. Partial correlation is a measure of functional connectivity that is more closely related to effective connectivity than simple correlation (Marrelec et al., 2007, 2009; Smith et al., 2011). It was computed in the same manner as integration [by using the 1000 samples of the Bayesian numerical sampling scheme, Marrelec et al., 2005, 2009]. The density of connections at a given threshold was computed as the number of ROI pairs for which partial correlation was above the threshold. A 'connectivity' curve was derived by computing the density of connections across a range of thresholds. Finally, the integral of the difference between two curves obtained under different conditions, hereafter referred to as integrated difference in partial correlation (IDPC), was computed. IDPC is independent from the partial correlation threshold and quantitatively estimates the differences in connectivity between conditions.

Due to the particular implication of fronto-parietal networks in conscious processes (see introduction and discussion), we wondered whether fronto-parietal interactions were specifically altered during propofol-induced unconsciousness. To do so, networks mentioned above were separated in their respective frontal, parietal, temporal, insular, occipital and cingulate components (Table S1). All these components were then considered as SOIs and used to compute integration and partial correlation measures. Only interactions between frontal and parietal areas (F-P), frontal and temporal areas (F-T) and parietal and temporal areas (P-T) were considered because only these areas were consistently represented in the detected networks. For these three types of interactions, both integration and partial correlations were computed within (e.g., between the frontal and parietal regions of one network) and between networks (e.g., between the frontal part of one network and the parietal parts of all other networks), whenever possible. 'Connectivity curves' were computed for each type of interaction, revealing their respective behaviour according to partial correlation in the wakefulness and deep sedation conditions. The IDPC was then computed for each type of interaction to measure any change in the F-P, F-T and P-T interactions between the considered conditions. To infer the significance of this difference in behaviour, a leave-one-out (LOO) scheme was performed: partial correlation was computed on all subjects except one to obtain connectivity measures and the process was repeated for each subject, leading to 12 curves of connectivity and IDPC. The results are presented in terms of the mean and standard deviation of these 12 measures. Connectivity curves obtained under different conditions (here, resting state wakefulness and deep sedation) were then compared for each threshold using a two-sample *t*-test on the 12 estimates population. Significance of the results concerning the IDPC was assessed using a paired *t*-test.

One could argue that ROI selection biased the assessment of functional connectivity since this measure was computed on regions selected from networks identified through sICA during a given state of consciousness (e.g., wakefulness). To account for this potential bias, we ran connectivity analyses on 3 different sets of ROIs:

Case 1 ROIs from the networks detected on all subjects in the wakefulness condition.

Case 2 ROIs from the networks detected on all subjects in the deep sedation condition.

Case 3 ROIs from the networks detected on half the population in the wakefulness condition. A first group (further referred to as selection 1) was composed of 6 of the subjects having 200 scans (chosen randomly from the 12 subjects) and the 6 subjects having 350 scans, only the first 150 scans of each run being considered. This group was used to select the ROIs. A second group (selection 2) was composed of the remaining 6 subjects having 200 scans and the 6 subjects having 350 scans, but considering the last 200 scans of each run. This group was used for interaction computations. The subdivision of the data as considered in case 3 was performed on a principled basis according to the following points: the two selections involved the same number of subjects to guarantee a similar weight to both data, the number of subjects in each selection was maximized, which led us to divide the larger sessions of 6 subjects and the selection used to compute interactions had to be balanced in terms of number of scans, to be comparable

between them.

Results

Whole brain analysis

Consistent with the literature, we identified six networks at the group level during resting wakefulness (Fig. S1, Damoiseaux et al., 2006; Perlbarg et al., 2008). Two were heavily loaded by primary or unimodal associative sensory or motor cortices, such as the visual (VIS) and the motor (MOT) networks. The others mainly consisted of multimodal associative cortices: the default mode (DM) network, the dorsal attentional (dATT) network, the ventral attentional (vATT) network and the salience (SAL) network.

Total integration was significantly (p<0.05) lower in the sedation condition than in the wakefulness condition in all systems of interest, namely at the brain and network levels (Fig. 2). This decrease in integration was associated with significant changes in both within-and between-system integrations. Within-network integration significantly decreased in all networks from wakefulness to deep sedation (Fig. 2, beige bars). Between-network integration also significantly decreased from wakefulness to sedation in most of the pairs of networks (Fig. 2, black bars and inset). However, vATT was an exception. There was no significant state-related change in integration between vATT and all other networks, except for the SAL network: the integration between vATT and SAL was significantly lower in sedation than during wakefulness.

Fig. 2. *Total integration decomposed in its within- (beige) and between-SOIs (black) components in the wakefulness (w) and deep sedation (s) conditions for the sum of all SOIs (Total) and for each SOI separately. All between-SOIs terms in the wakefulness (w) and deep sedation (s) conditions are detailed in the inset, by taking the symmetry of the terms into account Significant decreases in integration between the wakefulness (w) and deep sedation (s) conditions are marked by stars.*

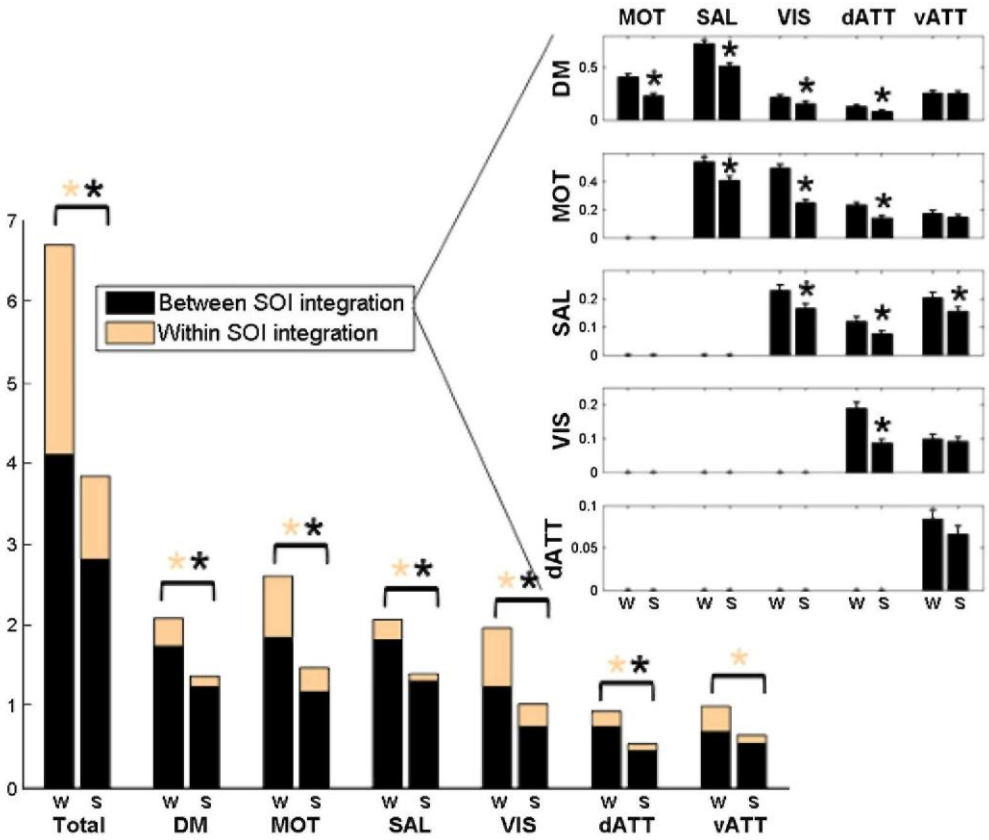

Fig. 3. *Integration within (beige) the frontal (F), parietal (P) and temporal (T) ROIs of a same network and between (black) the frontal (F), parietal (P) or temporal (T) ROIs of a network and the frontal (F), parietal (P) or temporal (T) ROIs of all other networks. Since vATT does not comprise any temporal region, there are no F-T or P-T results to display for this network. Significant decreases in integration between the wakefulness (w) and deep sedation (s) conditions are marked by stars.*

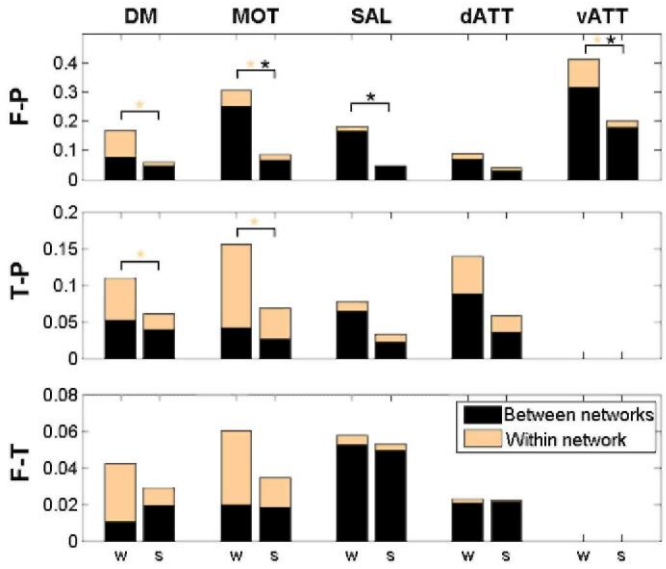

Fronto-parietal interactions during deep sedation

Integration

Integration measures between the wakefulness and deep sedation conditions were computed considering the relevant networks (i.e., all except VIS) separated in their frontal, temporal and parietal parts (Fig. 3, beige bars). The results revealed significant decreases from wakefulness to sedation in within-network integration between parietal and frontal areas (i.e., between frontal and parietal SOIs within a given network) in DM, MOT and vATT networks. The decrease in integration between frontal and parietal areas did not reach significance for the dATT and SAL networks. Concerning the parietotemporal interactions, integration decreased significantly from wakefulness to sedation only in the DM and MOT networks. Finally, none of the decreases in within-network integration were significant between the frontal and temporal SOIs of the considered networks.

Likewise, the integration between frontal and parietal areas across different networks decreased from wakefulness to sedation for the MOT, SAL and vATT networks (Fig. 3, black bars). None of the decreases in between-network integration were significant for temporo-parietal or fronto-temporal SOIs.

In summary, integration within or between networks was more often significantly decreased from wakefulness to sedation between frontal and parietal areas than between temporal and parietal areas or between frontal and temporal regions.

Partial correlation

To further specify the regional structure of changes in functional connectivity from wakefulness to deep sedation, we computed partial correlations, connectivity curves and IDPC separately for fronto-parietal, temporo-parietal and fronto-temporal areas.

In the connectivity curves, the average number of above threshold partial correlations between SOIs was significantly (p<0.05, corrected for multiple comparisons using the Bonferroni correction) smaller in the deep sedation condition than in the wakefulness condition for thresholds ranging from 0.03 to 0.19 for fronto-parietal SOIs, from 0.05 to 0.1 for fronto-temporal SOIs and from 0.04 to 0.16 for parietotemporal SOIs (Fig. 4a-c).

The integrated difference in partial correlation (IDPC) computed for each regional interaction (Fig. 4, shaded

green areas) revealed that the largest decrease in connectivity between the wakefulness and deep sedation conditions could be found between the frontal and parietal ROIs, followed by parieto-temporal ROIs and finally fronto-temporal ROIs (Fig. 4d). These differences in IDPC were all significant at $p<0.05$, corrected for multiple comparisons using the Bonferroni correction.

These results confirm a decrease in regional functional connectivity between frontal, parietal and temporal areas from wakefulness to deep sedation. They further suggest that the functional connectivity of parietal areas was more profoundly affected by anesthesia than that of frontal or temporal areas.

Fig. 4. *a-c: Average connectivity curves computed using all networks comprising regions in the lobes of interest (i.e., frontal and parietal in a, frontal and temporal in b and parietal and temporal in c) in wakefulness (blue) and deep sedation (red) conditions. X-axis: partial correlation threshold. Y-axis: connectivity level. The dashed black line shows the partial correlation interval for which the difference in connectivity between the wakefulness and deep sedation conditions was significant while the shaded green area on each plot represents the IDPC. d: Average IDPC with standard deviation from LOO scheme. Significant differences in IDPC are marked by stars.*

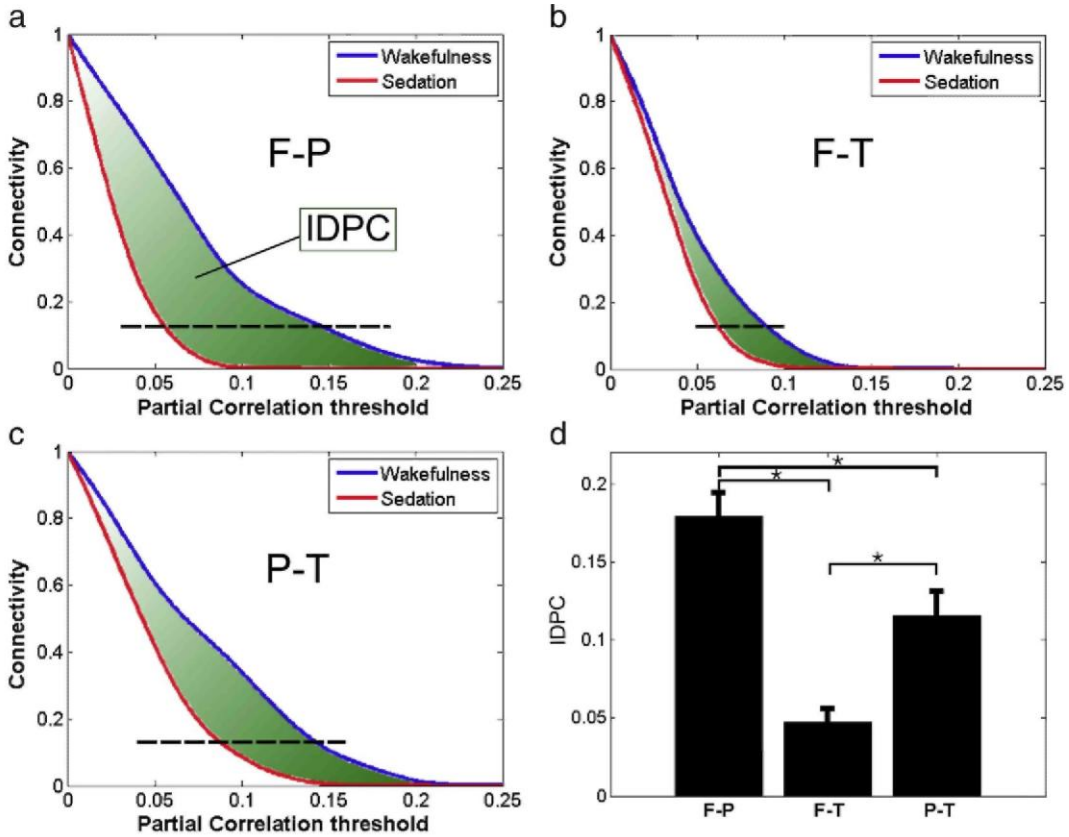

Influence of the ROI selection procedures

Differences were observed in terms of integration between the three samples tested with different ROI selection procedures (see Supplementary materials, Fig. S2): decreases in integration were significant when using one sample but became non-significant when using another (illustration: the decrease in integration between the vATT and DM SOIs was significant in case 1 but not in case 3). Case 2 even showed a significant increase in within-SAL integration while the other cases showed significant decreases from wakefulness to deep sedation. These results illustrate the potential bias induced by ROI selection. However, all cases showed a global decrease in both within-system and between-system integrations from wakefulness to deep sedation, which suggested that the effect of deep sedation on brain activity was larger than the potential bias induced by ROI selection. Although the bias inherent to ROI selection was found to be less important than the integration decrease between wakefulness and deep sedation, case 3 was selected to compute interactions (see all aforementioned results) to

limit the influence of this ROI selection bias.

Discussion and conclusions

Discussion

We tested the hypothesis that the loss of consciousness caused by propofol anesthesia is associated with a quantitative alteration in the capacity of the brain to integrate information, as estimated by two different parameters, integration and partial correlations. Results show that during deep sedation, total integration was significantly lower than during resting state wakefulness at the level of both the brain and its constituent networks. The decrease in integration was particularly consistent within each system (i.e., brain or networks). By contrast, integration between networks did not systematically decrease and the vATT network retained strong interactions with most other networks during deep sedation. Computation of partial correlations further suggested that functional connectivity was particularly affected between parietal areas and frontal or temporal regions during deep sedation. These findings support the important role of the parietal cortex in integrating information and sharing it with frontal associative areas, in a global workspace where conscious representations emerge.

The main finding of this study is the significant decrease in total integration at the brain and network levels from the wakefulness to the deep sedation condition. First, integration was systematically decreased within networks. During resting wakefulness, the activity coherently fluctuates in distributed sets of brain areas, which are therefore deemed to constitute functional networks (Fox and Raichle, 2007). In contrast, during deep anesthesia, the activity of areas within each network becomes more independent from one another and the exchange of information (in the Shannon's sense) is reduced. Second, integration also decreased between networks, for all networks except vATT. The maintenance of the integration between vATT and most other networks at resting wakefulness levels was unexpected and the mechanisms underlying this atypical behaviour remain uncertain. The vATT network is thought to serve as an alerting system that detects behaviorally relevant stimuli in the environment (Corbetta and Shulman, 2002). One can speculate that for this reason, interactions between vATT and the other networks are preserved even under conditions of lower consciousness. It is also possible that this peculiar connectivity pattern is related to structural connectivity. Indeed, diffusion spectrum imaging has identified the anterior cingulate, the precuneus and the inferior parietal cortex, which belong to vATT, as important hubs in the structural connectivity core of the human brain (Hagmann et al., 2008). In any case, the functional significance of this preserved connectivity is uncertain given that, as mentioned above, functional integration within vATT is significantly decreased.

The mechanisms underlying these effects are only partially identified. Propofol promotes GABA and weakly inhibits NMDA neurotransmissions (Kotani et al., 2008). GABAergic neurotranmission is the ubiquitous inhibitory neurotransmitter that shapes firing dynamics of neural ensembles (Traub et al., 1999). In contrast, NMDA neurotransmission is thought to be the main neurotransmitter of modulatory (so-called feedback) connections through which a brain area can be influenced by the activity of distant regions (Friston, 2005). It could be hypothesized that the modifications in neuronal firing patterns induced by propofol on two principal brain neurotransmitters are related to the modifications of brain integration observed at the systems level. However, a relationship between recorded BOLD signal and changes in neural cellular activity remains speculative.

In order to test the respective influence of interactions between parietal, frontal and temporal cortical areas in consciousness, we considered novel systems of interest, constituted of the relevant areas of the initial networks of interest. Results show that deep sedation was associated with reduced interactions between all these associative cortices. This finding suggests that coherent integration among frontoparietal cortices is important in the generation of conscious perception (Boly et al., 2008; Dehaene et al., 2006; Rees et al., 2002). However, as indicated by a larger decrease in IDPC, the functional interactions of parietal areas were deteriorated to a significantly larger extent than those of frontal or temporal areas. These results are consistent with the finding that activity impairment in posterior parietal areas is the most consistent correlate for loss of consciousness in severely brain damaged patients (Laureys et al., 2006; Vanhaudenhuyse et al., 2010), as well as in sleep and anesthesia states (Vogt and Laureys, 2005). They suggest a particular importance of connectivity in parietal cortices in conscious perception (Tononi and Laureys, 2008).

The functional consequences of the observed breakdown in brain integration during propofol-induced unconsciousness are far reaching. The flow of information is ubiquitously reduced between different specialized processors in a given network, which deprives them from the functional context usually provided by others

during resting wakefulness. This situation would result in a loss of the capacity of the brain to integrate information into a unique integrated conscious space and thus lead to the loss of consciousness that characterizes deep sedation. At present, the decrease of brain integration can be considered as a neural correlate of the loss of consciousness induced by sedation. However, the data only indicate that the deterioration of brain integration and a loss of consciousness are conditionally independent, given the administration of propofol. In our view, this result is not compelling enough to prove a causal link between the changes in brain integration and the state of consciousness, in the sense of causality developed by Pearl, 2000.

Conclusions

In conclusion, we used an objective and automatic methodology to hierarchically quantify integration within and between brain networks during anesthesia-induced loss of consciousness compared to wakefulness. We observed large and significant decreases in integration within and between networks as well as a fronto-parietal segregation in large-scale brain networks during deep sedation. These results suggest the importance of fronto-parietal areas in the generation of a conscious perception, and in particular, in this study, the potentially important role of a disruption of their integration for the generation of propofol-induced loss of consciousness.

Supplementary materials related to this article can be found online at doi: 10.1016/j.neuroimage.2011.04.020.

Acknowledgments

This study was supported by the Belgian Fonds National de la Recherche Scientifique (F.R.S.-F.N.R.S.), European Commission (Mind-bridge, DISCOS, CATIA and DECODER), Mind Science Foundation, James McDonnell Foundation, French Speaking Community Concerted Research Action (ARC 06/11-340), the Fondation Médicale Reine Elisabeth, the Research Fund of ULg, and PAI/IAP Interuniversity Pole of Attraction. J.S. is funded by a F.N.R.S. (Belgium) - Fonds pour la Recherche Industrielle et Agronomique (FRIA) grant; P.M., M.B., M-A B., A. V., S.L and C.P. are supported by F.N.R.S. (Belgium).

Appendix A. Regions, systems, and the brain

The material exposed in appendices A and B is thoroughly described in Marrelec et al., 2008.

In this section, we describe our notation regarding regions, systems, and associated time series, as well as our modeling hypotheses.

We first consider the N-dimensional fMRI BOLD time series $\mathbf{z}_t$, $t = 1,...,T$ associated with N regions of interest (ROIs) and assume that these time series are T temporally independent and identically distributed realizations of a N-dimensional random variable $\boldsymbol{y}$. Each ROI is therefore associated with a variable y_n, $n = 1,...,N$ and $\boldsymbol{y} = (y_1,...,y_N)$, standing for the joint variable, is associated to a probability distribution $p(\boldsymbol{y})$.

We further assume that ROIs are gathered into K systems of interest (SOIs). Each SOI, denoted by SOI_k, corresponds to the variable

$y_{SOIk} = (y_n)_{n \in SOIk}$.

Finally, the 'whole brain' level comprises all SOIs and, therefore, all ROIs. It does not correspond to the analysis of all the voxels of the brain but only refers to the top level of our hierarchy. This hierarchy is illustrated in Fig. 5.

Fig. 5. *Illustration of the hierarchical tree comprising the whole brain, K systems of interest (SOIs), and N regions of interest (ROIs). The top level is the level denoted 'whole brain' and is associated with total integration. Total integration is computed as the sum of K terms of within-SOI integration and one term of between-SOI integration. Both within- and between-SOI integrations are computed at the SOI level using the entropy of the ROIs, which is calculated at the bottom level of the hierarchy. Notations are explained in Appendix A*

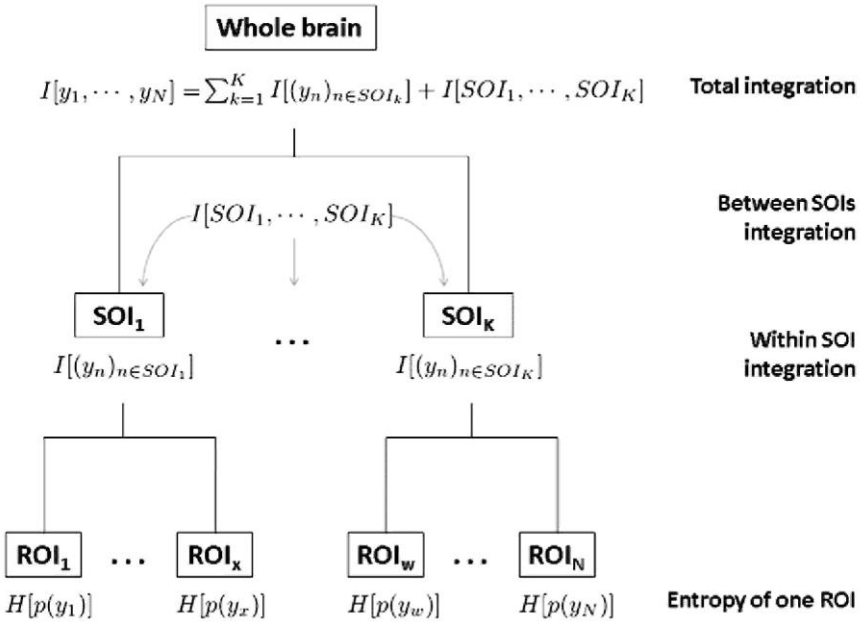

Appendix B. Hierarchical integration

An illustration of the hierarchy used to compute integration and which component can be derived at which level is exposed in Fig. 5. Within-SOI integration has the form:

$$\mathrm{I}\left[(y_{\mathrm{n}})_{\mathrm{n}\in\mathrm{SOI}_{\mathrm{k}}}\right]=\left[\sum_{\mathrm{n}\in\mathrm{SOI}_{\mathrm{k}}} H[p(y_{\mathrm{n}})]\right]-H\left[p\left(\mathbf{y}_{\mathrm{SOI}_{\mathrm{k}}}\right)\right] \qquad (1)$$

while between-SOI integration can be expressed as:

$$\mathrm{I}\left[\mathbf{y}_{\mathrm{SOI}_1},\ldots,\mathbf{y}_{\mathrm{SOI}_{\mathrm{K}}}\right]=\left[\sum_{\mathrm{k}=1}^{\mathrm{K}} H\left[p\left(\mathbf{y}_{\mathrm{SOI}_{\mathrm{k}}}\right)\right]\right]-H\left[p\left(\mathbf{y}_{\mathrm{SOI}_1},\ldots,\mathbf{y}_{\mathrm{SOI}_{\mathrm{K}}}\right)\right] \qquad (2)$$

Under the assumption of a Gaussian distribution of $\boldsymbol{y}$ with mean $\boldsymbol{\mu} = (\mu_n)$ and covariance matrix $\boldsymbol{\Sigma} = (\Sigma_{n,n})$, the entropy of one ROI can be written as:

$$H[p(y_{\mathrm{n}})]=\frac{1}{2}\ln\left[(2\pi e)\Sigma_{\mathrm{n,n}}\right] \qquad (3)$$

If $\boldsymbol{\mu}$ and $\boldsymbol{\Sigma}$ were known, within- and between-SOI integration could be derived from Eq (3). However, the true values of $\boldsymbol{\mu}$ and $\boldsymbol{\Sigma}$ are unknown and only partly accessible through the data. To infer the values of integration from the data, a Bayesian numerical sampling scheme that approximates the posterior distribution of the parameters of interest in a group analysis is performed (Marrelec et al., 2006). From there, all statistics can be easily obtained.

Appendix C. Statistics on the integration measures

The statistics are obtained from the 1000 samples integration values computed from the Bayesian sampling

scheme (see Marrelec et al., 2006 for details). In particular, it was possible to compute the posterior probability $p(A/\boldsymbol{y})$ of an assertion A (i.e. the total integration during sedation (Its) is larger than the total integration during wakefulness (Itw)) given the random variable $\boldsymbol{y}$ associated to the BOLD fMRI time courses of the considered ROIs. If p(Its > Itw) is close to 1, then one can confidently say that this statement is true, i.e., that Its > Itw. For practical purpose, a threshold of 0.95 was used. On the contrary, if p(Its > Itw) is close to 0, one can therefore state that Its<Itw. In the present case, p(Its > Itw) can be approximated by the number of times that total integration was found to be larger during sedation than during wakefulness in the 1000 samples, i.e.,

$$p(\text{Its} > \text{Itw}) \approx \#(\text{Its}_1 > \text{Itw}_1 : \text{I} = 1,...,L)/L$$

where # stands for the cardinal of a set (i.e., the number of elements in that set), and where $L = 1000$.

Since all tests are approximated simultaneously, all dependences are taken into account and no correction on the threshold is needed when considering one specific assertion (corresponding to marginal distributions).

References

Alkire, M.T., et al., 1995. Cerebral metabolism during propofol anesthesia in humans studied with positron emission tomography. Anesthesiology 82, 393-403.

Alkire, M.T., et al., 1999. Functional brain imaging during anesthesia in humans: effects of halothane on global and regional cerebral glucose metabolism. Anesthesiology 90, 701-709.

Alkire, M.T., Hudetz, A.G., Tononi, G., 2008. Consciousness and anesthesia. Science 322, 876-880.

Baars, B.J., 2005. Global workspace theory of consciousness: toward a cognitive neuroscience of human experience. Prog. Brain Res. 150, 45-53.

Boly, M., et al., 2008. Intrinsic brain activity in altered states of consciousness: how is the default mode of brain function? Ann. N.Y. Acad. Sci. 1129, 119-129.

Boveroux, P., et al., 2010. Breakdown of within- and between-network resting state fMRI connectivity during propofol-induced loss of consciousness. Anesthesiology 11, 1038-1053.

Corbetta, M., Shulman, G.L, 2002. Control of goal-directed and stimulus-driven attention in the brain. Nat. Rev. Neurosci. 3, 201-215.

Damoiseaux, J.S., et al., 2006. Consistent resting-state networks across healthy subjects. Proc. Natl. Acad. Sci. U. S. A 103, 13848-13853.

Dehaene, S., et al., 2006. Conscious, preconscious, and subliminal processing: a testable taxonomy. Trends Cogn. Sci. 10, 204-211.

Fox, M.D., Raichle, M.E., 2007. Spontaneous fluctuations in brain activity observed with functional magnetic resonance imaging. Nat. Rev. Neurosci. 8, 700-711.

Friston, K.A., 2005. theory of cortical responses. Philos. Trans. R Soc. Lond. B Biol. Sci. 360, 815-836.

Greicius, M.D., et al., 2004. Default-mode network activity distinguishes Alzheimer's disease from healthy aging: evidence from functional MM. Proc. Natl. Acad. Sci. U. S. A 101, 4637-4642.

Hagmann, P., et al., 2008. Mapping the structural core of human cerebral cortex. PLoS Biol. 6, 1479-1493.

Johnston, A.J., et al., 2003. Effects of propofol on cerebral oxygenation and metabolism after head injury. Br. J. Anaesth. 91, 781-786.

Kotani, Y., et al., 2008. The experimental and clinical pharmacology of propofol, an anesthetic agent with neuroprotective properties. CNS Neurosci. Ther. 14, 95-106.

Laureys, S., et al., 1999. Impaired effective cortical connectivity in vegetative state: preliminary investigation using PET. Neuroimage 9, 377-382.

Laureys, S., Boly, M., Maquet, P., 2006. Tracking the recovery of consciousness from coma. J. Clin. Invest. 116, 1823-1825.

Marrelec, G., et al., 2005. Conditional correlation as a measure of mediated interactivity in fMRI and MEG/EEG. IEEE Trans. Signal Process. 53, 3501-3516.

Marrelec, G., et al., 2006. Partial correlation for functional brain interactivity investigation in functional MRI. Neuroimage 32, 228-237.

Marrelec, G., et al., 2007. Using partial correlation to enhance structural equation modeling o functional MRI data. Magn. Reson. Imaging 25, 1181-1189.

Marrelec, G., et al., 2008. Regions, systems, and the brain: hierarchical measures of functional integration in fMRI. Med. Image Anal. 12, 484-496.

Marrelec, G., et al., 2009. Large-scale neural model validation of partial correlation analysis for effective connectivity investigation in functional MRI. Hum. Brain Mapp. 30, 941-950.

Martuzzi, R., et al., 2010. Functional connectivity and alterations in baseline brain state in humans. Neuroimage 49, 823-834.

Mhuircheartaigh, R.N., et al., 2010. Cortical and subcortical connectivity changes during decreasing levels of consciousness in humans: a functional magnetic resonance imaging study using propofol. J. Neurosci. 30, 9095-9102.

Pearl, J., 2000. Causality: models, reasoning and inference. Cambridge University Press.

Perlbarg, V., et al., 2007. CORSICA: correction of structured noise in fMRI by automatic identification of ICA components. Magn. Reson. Imaging 25, 35-46.

Perlbarg, V., et al., 2008. NEDICA: detection of group functional networks in fMRI using spatial independent component analysis. ISBI.

Rees, G., Kreiman, G., Koch, C, 2002. Neural correlates of consciousness in humans. Nat. Rev. Neurosci. 3, 261-270.

Smith, S., et al., 2011. Network modelling methods for fMRI. Neuroimage 54, 875-891.

Tononi, G., 2005. Consciousness, information integration, and the brain. The Boundaries of Consciousness: Neurobiology and Neuropathology, vol. 150. Laureys S.- Elsevier.

Tononi, G., Laureys, S., 2008. The neurology of consciousness. Academic Press.

Traub, R.D., Jefferys, J.G., Whittington, M.A., 1999. Fast oscillations in cortical circuits. MIT Press.

Vanhaudenhuyse, A., et al., 2010. Default network connectivity reflects the level of consciousness in non-communicative brain-damaged patients. Brain 133, 161-171.

Veselis, R.A, Feshchenko, V.A., Reinsel, R.A, Beattie, B., Akhurst, T.J., 2005. Propofol and thiopental do not interfere with regional cerebral blood flow response at sedative concentrations. Anesthesiology 102, 26-34.

Vogt, B.A., Laureys, S., 2005. Posterior cingulate, precuneal and retrosplenial cortices: cytology and components of the neural network correlates of consciousness. The Boundaries of Consciousness: Neurobiology and Neuropathology, vol. 150. Laureys S.- Elsevier.

White, N.S., Alkire, M.T., 2003. Impaired thalamocortical connectivity in humans during general-anesthetic-induced unconsciousness. Neuroimage 19, 402-411.

Zhang, H.Y., et al., 2009. Detection of PCC functional connectivity characteristics in resting-state fMRI in mildAlzheimer's disease. Behav. Brain Res. 197, 103-108.